ISPRS Annals of the Photogrammetry, Remote Sensing and Spatial Information Sciences, Volume XII-4/W1-2026
21st International 3D GeoInfo Conference 2026, 28–29 September 2026, Sofia, Bulgaria

A conceptual framework of 3D urban evacuation simulation under flooding: Integrating urban digital twins with agent-based modelling

Ruihang Xie[1], Fuko Nakai[1], Yoshihide Sekimoto[1]

[1] Center for Spatial Information Science, University of Tokyo, Tokyo, Japan - ruihang.xie@csis.u-tokyo.ac.jp; f-nakai@csis.u-tokyo.ac.jp; Sekimoto@csis.u-tokyo.ac.jp.

Keywords: 3D evacuation simulation, 3D city model, Evacuation modelling, Resilient city, Urban disaster prevention.

Abstract

Urban flood evacuation simulations commonly rely on two-dimensional (2D) representations of urban environments, even though real cities are inherently three-dimensional (3D). Because flood inundation is closely shaped by the 3D structure of urban space, this mismatch may bias estimates of evacuation feasibility and timing while limiting the evaluation of disaster response strategies. This paper therefore proposes a conceptual framework for 3D urban evacuation simulation under flooding by coupling an urban digital twin (UDT)-based 3D navigation network with an agent-based model (ABM). The navigation network represents multi-level navigable spaces and their connectivity as a 3D graph with mode-dependent constraints for walking, driving, and public transport. The ABM incorporates variables associated with the vertical dimension of evacuation processes. An illustrative example is provided to demonstrate the framework. The main contributions are: 1) a conceptual framework integrating UDTs and ABM for 3D urban evacuation simulation; 2) a hierarchical definition and specification of navigable spaces and their connectivity for constructing a 3D graph-based navigation network; and 3) the identification of variables for representing 3D evacuation processes. The framework helps enable more effective disaster prevention and response strategies.

1. Introduction

Many evacuations are advised to begin before hazards such as floods, tsunamis, or bushfires fully develop. The effectiveness of these evacuations fosters protecting lives and reducing losses. To support disaster prevention and response, many evacuation simulation models have been developed for urban contexts. From the perspective of disaster types, most existing models focus on hazards such as hurricanes (Adjei *et al*., 2022), tsunamis (Mostafizi *et al*., 2017), and earthquakes (Chang *et al*., 2022), with a growing number of studies addressing wildfires (Siam *et al*., 2022) and other hazards (e.g., bombs, nuclear) (Yang *et al*., 2020). With increasing risk of climate change, some models (Nakai, *et al*., 2026; Roy *et al*., 2022; Yang *et al*., 2025) have been developed for floods. For examples, Mizumura *et al* (2024) developed a multi-agent simulation to show that, under delayed decisions and dynamic flood conditions, evacuating inundated areas via the shortest feasible route can reduce evacuation time.

Current simulation models rely on fundamentally two-dimensional (2D) representations of urban environments or 2.5D with elevation/slopes, treating people motions as occurring on a planar surface. In fact, common people motion modes (walking, driving, and public transport) in cities are inherently three-dimensional (3D). People are distributed across underground, ground-level, and elevated spaces, including deep subway stations, high-rise buildings, and interconnected transport infrastructures. Even individuals sharing the same horizontal location (x, y) may face significantly different evacuation conditions depending on their vertical position, movement direction (descending, horizontal, or ascending), and access to vertical circulation spaces such as stairs, escalators, or lifts. This is particularly evident in complex multi-level transport hubs such as Shibuya Station in Tokyo.

Moreover, flood inundation and evacuation options are significantly height dependent. Inundation propagates along low-lying areas (e.g., underground spaces), while higher elevations (e.g., high-rise buildings) may remain safe for longer periods. As flood depth and flow conditions evolve, low-elevation routes may rapidly lose accessibility, whereas upward movement may remain feasible and become the dominant safety strategy (Lv *et al*., 2025). Thus, understanding urban evacuation under flooding as a spatiotemporal process unfolding in 3D space benefits improving the realism of evacuation assessment and disaster response levels.

Recent advances in urban digital twins (UDTs) have significantly improved the availability of large-scale 3D city models (Lei *et al*., 2023), while agent-based modelling (ABM) has matured as a powerful approach for representing heterogeneous behaviours, adaptive decision-making, and interactions between individuals and environments (Xie *et al*., 2022). These developments create new opportunities to move beyond 2D assumptions and to model evacuation as a 3D, behaviourally rich, and spatially explicit process at the urban scale.

Accordingly, this study proposes a conceptual framework for 3D urban evacuation simulation that integrates UDTs with ABM. The framework systematically defines how 3D navigable spaces are classified, represented, and connected, and how evacuation behaviours are operationalised in 3D space. The focus of this study is on conceptual and methodological formulation rather than full system implementation and development. The main contributions of this paper are: 1) a conceptual framework integrating UDTs and ABM for 3D urban evacuation simulation under flooding; 2) a hierarchical definition and specification of navigable spaces and their connectivity in 3D urban environments to support the construction of a 3D graph-based network; and 3) the identification of key variables required for an ABM to represent 3D urban evacuation processes.

2. Related works

This section reviews the key background and gaps in space classification for navigation and evacuation and ABM for urban evacuation simulations.

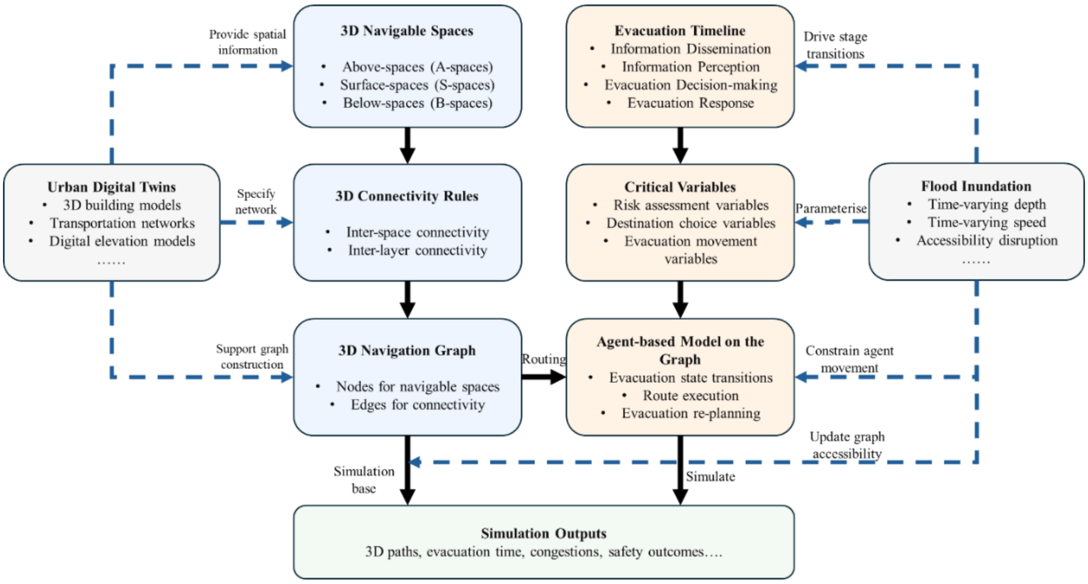

Figure 1 Conceptual framework of the 3D urban evacuation simulation under flooding.

2.1 Space classifications for navigation and evacuation

From the perspective of navigation and evacuation, urban space has been classified in various ways. CityGML, for example, distinguishes urban physical space into occupied and unoccupied space. Occupied space refers to volumetric entities that physically fill space, such as buildings, walls, and structural elements, whereas unoccupied space refers to volumetric entities representing free space not occupied by physical matter and therefore potentially available for movement (OGC Consortium, 2021). In addition, more practical classifications have been proposed to bridge outdoor and indoor environments. Within outdoor space, road space is among the most frequently discussed categories. Road space is a general term for spaces used for transportation (Zlatanova *et al*., 2020). Semantics-based approaches further classify outdoor navigable spaces according to their functional meaning, such as roads, sidewalks, and crosswalks (Karimi and Kasemsuppakorn, 2013). More refined schemes introduce intermediate categories, such as semi-indoor and semi-outdoor spaces, to capture transitional morphologies including arcades, covered walkways, and atria open to the exterior (Kray *et al*., 2013; Wang *et al*., 2023, Yan *et al*., 2019).

Within indoor navigation research, IndoorGML 2.0 formalises a navigation-oriented distinction by categorising space cells into *NavigableSpace* and *NonNavigableSpace* (Diakité *et al*., 2020). Most studies also adopted such similar classification. However, indoor environments often contain spaces that are not cleanly separable under a strict binary classification. Notably, Diakité and Zlatanova (2018) subdivided indoor space into object space (O-space), functional space (F-space), and remaining space (R-space). Recent research (Xie *et al*., 2024; Xie *et al*., 2023) has introduced space components based on 3D pedestrian motions (e.g., low crawling, jumping up/down) through freely navigable spaces, navigable spaces under conditions, and non-navigable spaces.

Some studies (Bruyns *et al*., 2020; Guler, 2024; Karabin *et al*., 2020; Sun *et al*., 2019) mention concepts analogous to “above” and “below” spaces in urban context, but these notions are often treated as descriptive terms rather than being formalised within a consistent space classification framework that supports 3D urban evacuation simulation. Therefore, a classification is needed to identify which types of navigable spaces are evacuation-relevant, what roles they perform, and which attributes should be retained to support behavioural simulation.

2.2 Agent-based models for urban evacuation simulations

In flood evacuation research, ABMs are particularly suitable for representing behavioural heterogeneity because agents can be parameterised with distinct attributes and decision rules. For example, Lv *et al* (2025) integrated ABM with hydrodynamic simulation to examine how transport modes, shelter configurations, and flood-affected road networks influence evacuation efficiency. Shu *et al* (2025) developed a dynamic flood risk assessment framework that couples a hydrological–hydrodynamic model with an ABM of evacuation and evolving vulnerability. Despite their contributions, such models generally operate on 2D road networks and do not support the representation of key 3D mechanisms, such as floor-dependent exposure and accessibility, vertical circulation constraints.

A limited number of studies (León *et al*., 2025; Mostafizi *et al*., 2019; Yang *et al*., 2025) have introduced vertical evacuation into ABMs. For instance, Mostafizi et al (2019) proposed a tsunami evacuation simulation, showing that shelter location nonlinearly shapes both the proportion of vertical evacuees and overall mortality. While such studies provide valuable insights, verticality is commonly operationalised as a simplified “move-up” action to a designated shelter, rather than being embedded across the full evacuation timeline or linked to explicit multi-level navigable spaces (e.g., deep underground environments and their access constraints). In addition, although indoor-focused 3D ABMs can model detailed 3D motions (e.g., low crawling, jumping up/down) and microscopic interactions (Xie *et al*., 2025a; Xie *et al*., 2025b; Xie *et al*., 2025c), they are not directly transferable to urban contexts.

3. A conceptual framework

As shown in Figure 1, the framework consists of two components. On the left, UDTs are used to obtain the 3D navigation network through the specification of 3D navigable spaces, connectivity rules, and the resulting 3D navigation graph. On the right, flood inundation and its simulation influences the evacuation timeline, the definition of critical variables, and the operation of the ABM on the graph. The two components are linked through the navigation graph. Their interaction ultimately produces the simulation outputs (e.g., 3D evacuation paths, evacuation time, congestion, and safety outcomes).

3.1 3D navigation network based on UDTs

We define the classification of navigable spaces and then specify their connectivity within the 3D urban navigation network.

3.1.1 Definitions of 3D navigable spaces

Before constructing the 3D navigation network, 3D navigable spaces should be defined for urban evacuation simulation under flooding. The core elements that determine urban evacuation feasibility are: a) where agents can enter or leave above-/below-ground interiors, b) how they change elevation, and c) how they transfer into the broader transportation network. Based on these, we adopt a two-tier classification scheme. At the primary level, 3D navigable spaces are classified into:

- Above-spaces (A-spaces): A type of navigable space located within above-ground interior areas or elevated facilities that does not form part of the surface transportation network, but enables evacuees to access, exit, or move within that network. These spaces correspond to evacuation circulation spaces that direct evacuees from indoor areas towards safe areas (e.g., evacuation stairwells and exits). Function-specific enclosed rooms that do not contribute to circulation, such as office rooms, toilets, storage rooms, service rooms, and similar spaces, are excluded.
- Surface-spaces (S-spaces): A type of navigable spaces that form the primary surface transportation network and are traversable as a continuous surface-connected manifold, in which evacuees can use walking, driving, or public transport. A space is classified as an S-space if it supports uninterrupted network connectivity via continuous movement and does not require discrete floor/height transitions. Examples include streets, pavements, and open squares.
- Below-spaces (B-spaces): A type of navigable spaces located in underground interior facilities that is not part of the surface transportation network, but is used by evacuees to access, leave, or move between that network. These spaces correspond to evacuation circulation spaces that direct evacuees from underground occupied areas towards safe areas (e.g., evacuation stairwells, exits, and lifts). Like A-spaces, function-specific enclosed rooms are excluded.

Following previous studies (Kray *et al*., 2013; Wang *et al*., 2023), we further classify A-spaces and B-spaces according to their functional role at the secondary level:

- Transitional spaces (A_T-spaces, B_T-spaces, AB_T-spaces): navigable spaces that provide access between A-spaces or B-spaces and S-spaces, such as building exits.
- Vertical circulation spaces (A_V-spaces, B_V-spaces): navigable spaces that enable movement between different elevation levels within A-spaces or B-spaces, such as stairways, escalators, lifts, and other vertical connectors.

Detailed within-floor horizontal circulation (e.g., corridors and lobbies) and other non-circulation indoor spaces, such as rooms or function-specific areas are not represented in the navigation model, because the proposed model focuses on urban-scale navigable structure. Based on the above definitions, Figure 2 presents schematic examples of A-, S-, and B-spaces and their secondary functional subtypes, thereby illustrating the proposed two-tier classification scheme.

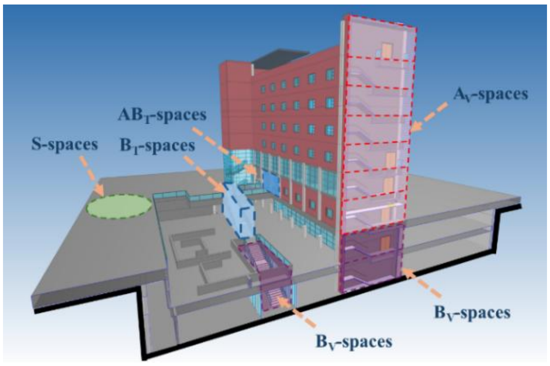

Figure 2 Schematic examples of the proposed classification of 3D navigable spaces.

3.1.2 Specifications of navigable spaces

1) A-spaces and B-spaces

For graph construction, an A- or B-space node is identified based on three key factors: a) spatial location, b) semantics, and c) adjacent spaces. First, a space is classified as an A_T/B_T/AB_T-spaces if:

a) it is located on a specific/single floor;
b) it has the semantics of a door, entrance, exit, or exit-related access space; and
c) it is adjacent to at least two connected spaces, including one outdoor space and one indoor space.

Condition a) ensures that the space is instantiated as a floor-specific element in the 3D graph. Condition (b) provides the semantic basis for identifying it as a formal exit or access element. Condition (c) provides the topological basis for distinguishing genuine transitional spaces from internal doors. A transitional space is then classified as an A_T-space, B_T-space, or AB_T-space according to whether the connected indoor circulation space belongs to an A-space, a B-space, or both. In some cases, a transitional space may serve both A-spaces and B-spaces simultaneously. Such spaces are represented as shared transitional spaces, i.e., AB_T-spaces (see Figure 3).

(a) (b) (c)

Figure 3 Examples of transitional spaces. (a) A_T-space (dark blue). (b) B_T-space (purple). (c) AB_T-space (light blue).

Second, a space is identified as an A_V/B_V-space if:

a) it has the semantic of a vertical circulation component, such as stairs, ramps, lifts (cannot be used under fire scenarios), or escalators;
b) it connects at least two distinct floors; and
c) its vertical location is above or below the ground surface.

Condition (a) provides the semantic basis for distinguishing A_V-spaces from other spaces by restricting them to explicit vertical circulation components. Condition (b) ensures that the space functions as an inter-floor connector rather than as a floor-specific access point. Condition (c) distinguishes A_V-spaces from B_V-spaces. In the 3D graph, the same vertical circulation component (e.g., a stairwell) is represented separately at each served floor and can be connected to its adjacent-floor counterparts. For example, the stairwell associated with a given floor is represented as an A_V-/B_V-space and its corresponding node. Under the scenario of a vertical circulation component directly adjacent to the outdoor transportation network, the space of the staircase (or escalator/lift) connecting to the ground is modelled as an A_T-space, B_T-space, or AB_T-space, because it realises a discrete level transition and connects to S-spaces. An A- or B-space node may support either walking or driving, depending on its functional role. For example, spaces within multi-storey car parks may permit vehicular movement in addition to pedestrian movement.

2) S-spaces
An S-space is specified as a surface-network node if all of the following conditions are met: a) it belongs to a transportation road or a surface-access point within the surface transportation network; b) it has route-related semantics indicating at least one permitted motion mode (e.g., driving, or public transport access); and; c) it forms a topological connection in the network, including a route intersection, route endpoint, or a surface-access point connected to an A-space or B-space.

Condition (a) ensures that the space is part of the navigable transportation substrate rather than a generic outdoor area. Condition (b) provides the semantic basis for assigning mode permissions and access constraints. Condition (c) provides the topological basis for instantiating graph nodes only at locations where network connectivity is operationally meaningful. The attributes of S-spaces can describe the motion modes at each node location. Walking is permitted in S-spaces accessible to pedestrians, such as pavements and pedestrian streets; driving is permitted in S-spaces accessible to vehicles, such as general roads; and public transport is permitted in S-spaces designated for public transport routes, such as bus or tram lines.

3.1.3 Specifications of navigable space connectivity

Let $G = (V, E)$ be the 3D navigation graph, where each node $v \in V$ is an A-, S-, or B-space node, and each edge $e = (v_i, v_j) \in E$ denotes a connection. An edge $e = (v_i, v_j)$ is valid for a motion mode m only if both endpoints permit m, and the edge type itself supports m (e.g., a public-transport edge must lie on a designated public-transport route).

1) Inter-space connectivity
For S-spaces, edges are created between adjacent S-space nodes according to route-map connectivity. Regarding A-spaces and B-spaces, edges are created between their relevant nodes that belong to the same floor and are physically and topologically adjacent. This abstraction reduces network complexity under limited data availability while preserving essential navigability. Such connections include linking A_T-/B_T-/AB_T- nodes to their nearest A_V-/B_V nodes. For each vertical circulation node in A_V-/B_V-spaces, vertical edges are created to connect its floor-specific instances across adjacent floors, thereby representing motions between discrete floor levels. The allowed mode is walking, and directionality is bidirectional unless restricted.

2) Inter-layer connectivity
To couple A-spaces and B-spaces with S-spaces, each valid access interface is linked to the surface transportation network at its actual attachment location. This is because an exit in reality typically connects to a surface route segment (e.g., a pavement edge or roadside access line). To avoid graph fragmentation, an attachment tolerance ε_a is suggested. Operationally, for each A_T-/B_T-/AB_T-space node, the nearest or corresponding eligible surface-network edge is first identified. If the location lies within ε_a of an existing surface edge and the offset is negligible at the adopted graph resolution, the A_T-/B_T-/AB_T-space node is treated as directly attached to the surface network, and no additional inserted S-space node is required (see Figure 4a). By contrast, if the distance exceeds ε_a, the access location is projected onto the corresponding surface-network edge, a surface-access S-space node is inserted at the projected position, and the original edge is split so that the inserted node becomes part of the surface network topology. A short transition edge is then created between the A_T-/B_T-/AB_T-space node and the corresponding surface-access S-space node. This ensures that above-ground or below-ground exits connect to the surface route itself (see Figure 4b).

(a) (b)

Figure 4 Illustrations of inter-layer connectivity between A-/B-spaces and S-spaces. (a) An A_T-space node is directly attached to the surface network when the connection location is within the attachment tolerance ε_a. (b) When the distance exceeds ε_a, a transition edge is created to a surface-access S-space node. Green denotes the S-space edge and node; blue denotes the transition edge and A_T-space node.

The allowed modes for edges are determined by the functional role of the access interface. Walking is always permitted. Driving is permitted only when the access point is explicitly vehicle-accessible (e.g., a parking-related ramp or vehicle entrance). Public transport is permitted only when the access point is functionally linked to a designated transit facility.

3.2 3D evacuation simulation based on ABM

ABM offers a computational framework for 3D urban evacuation simulation. We first establish an evacuation modelling timeline grounded in behavioural theories, then identify a set of critical variables that capture the role of the vertical dimension and finally suggest how these variables are incorporated into an ABM.

3.2.1 Evacuation modelling timelines

The Protective Action Decision Model (PADM) provides the theoretical basis for the evacuation timeline in this study, as it captures the sequential process of risk interpretation and protective response and has been widely applied to hazards such as floods, wildfires, and earthquakes (Lindell and Perry, 2012). Building on PADM and prior studies on flood evacuation behaviour, the timeline is structured into four components: information dissemination, information perception, evacuation decision-making, and evacuation response. Evacuation may be triggered by official warnings, environmental flood cues, or social cues, depending on hazard conditions and warning availability (Maranzoni *et al*., 2023; Ringo *et al*., 2024; Ryan, 2018). Once cues are disseminated, individuals may receive, attend to, and understand them, while perceived risk evolves dynamically and influences the likelihood of response (Roy et al., 2022). If evacuation is considered necessary, decision-making then involves risk assessment, destination choice, transport mode choice, and route choice (Roy *et al*., 2022; Wang *et al*., 2021; Yuan *et al*., 2017). Finally, evacuation response includes social coordination, preparatory activities, and movement through

https://doi.org/10.5194/isprs-annals-XII-4-W1-2026-309-2026 | © Author(s) 2026. CC BY 4.0 License.

complex urban environments, during which evacuees may continue to adjust routes, destinations, and transport modes as conditions change (Lindell *et al*., 2019; Liu *et al*., 2012).

3.2.2 Identification of critical variables

To operationalise the evacuation timeline in 3D space, each agent is embedded in the 3D navigation graph G by mapping its initial location to a valid A-/S-/B-space node that preserves where it is before an evacuation starts. All evacuation actions are executed on G subject to mode validity and dynamic accessibility under flooding. The critical variables define below are evaluated with respect to the agent's current node and feasible paths in G.

1) Evacuation decision-making stage

a) Risk assessment

First, risk assessment at this stage can be influenced by factors such as message clarity, proximity to the hazard source, and the visibility of environmental cues (Kakimoto and Yoshida, 2022; Weller *et al*., 2016). Although the technical flood risk concept of hazard–vulnerability–exposure is formulated for area-based assessments (Koks *et al*., 2015), these three components conceptually align with how evacuees can subjectively and logically analyse danger: flood intensity corresponds to hazard, personal physical and social characteristics reflect vulnerability, and spatial location represents exposure. In this respect, the vertical dimension plays a critical role in assessed exposure: residents on ground floors tend to overestimate flood probability (de Wolf *et al*., 2024) and think they have higher immediate threat than upper-floor occupants (Morss *et al*., 2016).

Specifically, an expected impact variable $EI_{i(t)}$, scaled to [0, 1] is suggested to represent each individual's assessed impact of the flood on itself or its dependents (e.g., children, older parents) at time *t*. Larger values indicate more severe expected consequences. Following previous studies regarding urban flood risk assessment (He *et al*., 2025; Luo *et al*., 2024), the expected impact is computed as:

$$EI_{i(t)} = H_{i(t)} * V_i * E_i \tag{1}$$

where $H_{i(t)}$ represents flood hazard within an agent's assessment radius *r* for itself or its dependent agents at time *t*; V_i denotes an agent's vulnerability for itself or its dependents; E_i captures the extent to which an agent *i* or its dependents is physically exposed to floodwaters, with a consideration on vertical position from the surface network and typical building structure that they are currently located. E_i can be defined by $E_i = f(VP_i, BS_i, X_i)$, where VP_i is a vertical-position factor [0,1]. For example, 1.0 for underground locations (e.g., subway, basement), 0.5 for ground level, and 0.2 for higher floors; BS_i is a building structure factor [0,1], reflecting the capability of the structure; X_i denotes additional optional exposure-related factors.

The variable $EI_{i(t)}$ is suggested to be against a frequently discussed factor, i.e., perceived risk level PRL_i. If $EI_{i(t)} \geq PRL_i$ is met, the individual can proceed to evacuation decision-making phase. Otherwise, the individual remains static and continues to update $EI_{i(t)}$ over time.

b) Destination choice

According to existing studies (Adjei *et al*., 2022; Wang *et al*., 2021), destination choice can be influenced by multiple factors, including transportation accessibility, risk, socio-demographic and economic characteristics, and the availability of accommodations, etc. Vertical dimension also plays a critical role; for example, evacuees typically prioritise to select higher destinations (Morss *et al*., 2016). Once an individual decides to evacuate and remain within the current city, it may select among four destination types: home, public shelter, shelter-in-place, or other destinations (e.g., friends' homes or hotels). For each potential destination type *j*, a utility value U_{ij} can be computed as a simple illustrative form at this stage to reflect the overall attractiveness of destination type *j* for agent *i*:

$$U_{ij} = \beta_0 + \beta_{TD}(-TD_{ij}) + \beta_{BH}BH_j + \beta_{BS}BS_j + \beta_{AC}AC_j + \beta_{PP}PP_{ij} \tag{2}$$

where TD_{ij} is travel distance, BH_j is building height, BS_j is building structural capability, AC_j represents accommodation conditions, and PP_{ij} captures personal preference (influenced by age, financial status, mobility, household structure, etc.). Among these, BH_j and BS_j directly encode the effect of the vertical dimension, while the remaining terms preserve behavioural realism in destination selection. Destination type selection probability can then be represented using a multinomial logit model $P(DT_i = j) = \frac{e^{(U_{ij})}}{\Sigma_k e^{(U_{ik})}}$. Once the destination type is determined, an agent can select a specific destination of that type around it.

2) Evacuation response stage

Afterwards, evacuation movement stages further consider variables regarding 3D (see Section 4.1). At this stage, vertical dimension influences evacuation in two ways. First, it affects the time required for each agent to reach S-spaces, because agents in A-spaces or B-spaces perform additional vertical movement (e.g., stair climbing) and some of them may experience higher congestion in high rise buildings or subways stations. Second, it affects their effective evacuation speed in early stages, as vertical movements are generally slower and more constrained in B-spaces due to higher possibility of physical fatigue. Once an agent has entered an S-space, however, its movement is treated as horizontal and modelled using a mode-dependent speed. When an agent arrives at its final destination (e.g., a public shelter), it is regarded as safe, and any further vertical movement inside the destination building (e.g., moving to upper floors) is not simulated. This internal vertical redistribution does not change the agent's safety status. Thus, an indoor evacuation time variable $IT_i(t)$ is introduced to represent the time required for agent *i* to reach the surface transportation network when initially located in A-spaces or B-spaces. $IT_i(t)$ is computed by local pathfinding on the facility-level A/B subgraph of the 3D navigation graph. Specifically, for agent *i* at time t, let $P_i^*(t)$ denote the minimum-time path from the agent's current node to a valid surface-access interface. The indoor evacuation time is then defined as the cumulative travel time along this path:

$$IT_i(t) = \sum_{e \in P_i^*(t)} \tau_{i,e}(t) \tag{3}$$

where $\tau_{i,e}(t)$ is the time cost of traversing edge e at time t. Once an agent reaches a surface-access nodes, it navigates to its destination on the surface transportation network according to its selected transport mode and chosen route.

4. Demonstration of the conceptual framework

We present a district-scale scenario using a university campus. This illustration is intentionally conceptual. The focus is on the resulting space configuration and graph structure rather than on the automation of extraction. As shown in Figure 5a, the campus represents a compact urban block in a metropolitan flood

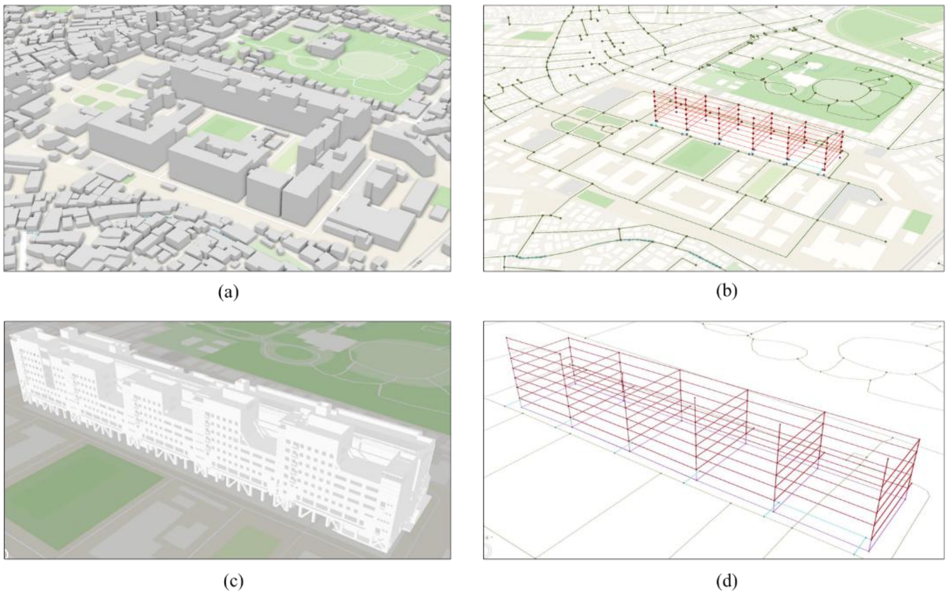

Figure 5 (a) 3D city model of the campus. (b) Identified 3D navigation network of the university campus. (c) Selected high-rise building for the 3D illustration. (d) Identified 3D navigation network within a building. A_V-spaces, AB_T-spaces, B_V-spaces, and S-spaces, together with their corresponding edges, are shown in red, blue, purple, and green, respectively.

evacuation context. The datasets used in this study were obtained from OpenStreetMap and PLATEAU 3D City Model.

Based on the definitions in Section 4.1, navigable spaces and their connectivity were instantiated and labelled in the 3D model as shown in Figure 5b. A_V-spaces, AB_T-spaces, B_V-spaces, and S-spaces, together with their corresponding edges, are shown in red, blue, purple, and green, respectively. S-spaces and their connectivity formed the primary interface of the transportation network and were represented as a 2D graph of nodes and edges, including intersections and continuous route segments, with green points and polylines denoting nodes and edges, respectively. A-spaces were instantiated in a selected high-rise building, where they enable agents to descend towards S-spaces (see Figure 5c). Finally, inter-layer transitions were established by connecting the AB_T-spaces of the building to the nearest corresponding edges of the transportation network, thereby creating explicit A↔S and B↔S interfaces through which agents can enter the surface transportation network (see Figure 5d).

For illustration, we present an example with walking and driving modes for the scenario. The aim is not to claim an implemented routing engine, but to demonstrate that the 3D space categories and connectivity rules yield more defensible evacuation than those derived from a 2D surface-only abstraction. A helper agent was initialised on Floor 5 of the selected building, as shown in Figure 6a. Once evacuation was triggered following risk assessment, the agent first travelled to pick up two dependents and then returned to their home near the campus for sheltering. In the 3D representation, the agent's vertical position was preserved, requiring a vertical transition and thereby introducing non-negligible constraints on both travel time and route feasibility.

Its 3D route consists of a pickup stage and an evacuation stage (see Figure 6a):

a) Pickup routes
   - It descended through A_V-spaces on foot to reach an exit node in the AB_T-space.
   - It traversed an AB_T↔S transition edge on foot to the corresponding S-space access point.
   - It then travelled along S-space edges on foot to the pickup location.

b) Evacuation routes
   - After picking up the two dependents, they walked along S-space edges to a car park within the campus.
   - They then drove out of the campus and return home for sheltering.

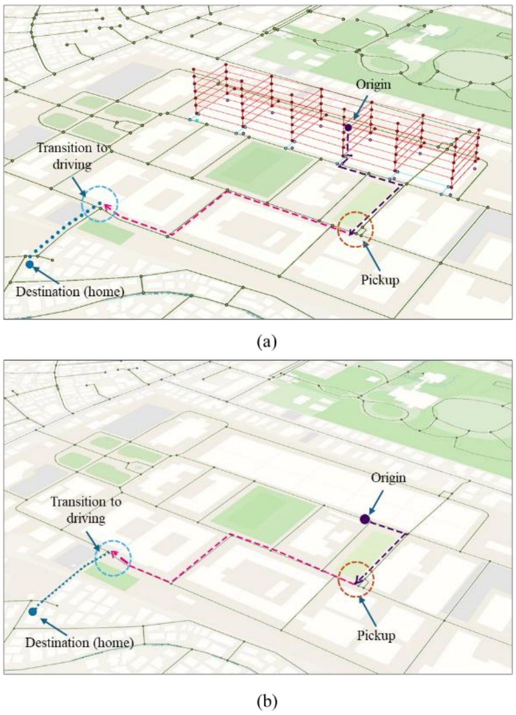

Figure 6 Illustrative routes from origin to destination. (a) 3D routes; (b) 2D routes. Pickup routes by walking, evacuation movement routes by walking, evacuation movement routes by driving are coloured with purple dashed lines, pink dashed lines, and blue dotted lines.

By contrast, in a 2D representation, the origin was typically projected onto the nearest surface node, implicitly assuming

https://doi.org/10.5194/isprs-annals-XII-4-W1-2026-309-2026

immediate access to the surface network through pre-evacuation time (Figure 6b). Consequently, two agents sharing the same horizontal (x, y) but occupying different heights (e.g., concourse vs platform) can have different IT_i, different earliest arrival times to S-spaces through our developed framework, and therefore different feasible route sets under dynamic conditions.

5. Discussion and conclusion

This study advances the methodological basis for 3D urban evacuation simulation under flooding by proposing a conceptual framework that couples a UDTs-based 3D navigation network with an ABM. The central contribution is a coherent operational logic that links (a) how multi-level urban navigable spaces are represented and connected for urban evacuation simulation, and (b) how agents' decisions and movements evolve in response to flood-driven accessibility changes. In this sense, the framework addresses a current gap in the literature, which is that many urban evacuation models remain fundamentally 2D. This study is expected to answer how 3D verticality can influence disaster response and prevention strategies.

The navigation component introduces graph-based modelling choices. In particular, the inter-layer connectivity based on surface-access S-space nodes resolves a common but under-discussed modelling error in current simulation models: building/underground exits do not naturally connect to road intersections, but to route segments. By inserting or assigning surface-access nodes on eligible surface edges, the framework preserves network topology and avoids artificial long connector edges that can bias travel-distance estimates and route choice. The additional rule that A_T-/B_T-/AB_T-space nodes may serve as direct surface-access interfaces captures real urban cases. A key methodological implication concerns where the vertical dimension matters most in flood evacuation. The framework formalises that verticality influences evacuation through two coupled mechanisms: (1) exposure and feasibility in evacuation decision-making, and (2) additional time costs and constraints in evacuation movement. This offers a principled explanation for why surface-only representations can systematically underestimate early-stage delays, mischaracterise route feasibility, and distort the timing of evacuation effectiveness. The demonstration is conceptual though, yet it makes explicit which elements should exist in the representation for 3D evacuation to be meaningful (e.g., vertical connectors, inter-layer access).

Nevertheless, the present framework does not model detailed within-floor horizontal circulation. This is appropriate for city-scale feasibility and for illustrating the impact of vertical position and vertical transitions; however, it may under-represent building-internal bottlenecks in critical facilities (e.g., major stations, malls). A possible extension is a multi-resolution strategy in which the 3D navigation graph retains the current abstraction while selected facilities are refined with higher-resolution internal graphs. The framework presumes that the necessary information for identifying exits and vertical circulation components can be obtained from UDTs. In real cities, data incompleteness and inconsistencies remain a major barrier. Future work will focus on:

1) Developing automated procedures to generate the 3D urban navigation graph from UDTs datasets.
2) Implementing and extending the ABM to support dynamic decision-making and adaptive movement on the 3D graph under time-varying flood impacts.
3) Validating the resulting model through sensitivity analysis and comparison against observed mobility patterns in floods.

Acknowledgements

This work was supported by Council for Science, Technology and Innovation (CSTI), Cross-ministerial Strategic Innovation Promotion Program (SIP), Building a Smart Infrastructure Management System (Funding agency: Public Works Research Institute), and by the Japan Science and Technology Agency (JST; Grant No. JPMJMI24I1).

References

Adjei, E., Murray-Tuite, P., Ge, Y., Ukkusuri, S. and Lee, S., 2022. Estimating hurricane evacuation destination and accommodation type selection with perceived certainty variables. *Transp Res D Transp Environ*, 105: 103235.

Bruyns, G.J., Higgins, C.D. and Nel, D.H., 2020. Urban volumetrics: from vertical to volumetric urbanisation and its extensions to empirical morphological analysis. *Urban Stud*., 58(5): 922-940.

Chang, K., Wu, Y. and Ke, S., 2022. A simulation-based decision support tool for dynamic post-disaster pedestrian evacuation. *Decis. Support Syst*., 157: 113743.

de Wolf, L.A., Robinson, P.J., Botzen, W.J.W., Haer, T., Mol, J.M. and Czajkowski, J., 2024. Factors of influence on flood risk perceptions related to Hurricane Dorian: an assessment of heuristics, time dynamics, and accuracy of risk perceptions. *Nat. Hazards Earth Syst. Sci*., 24(4): 1303--1318.

Diakité, A.A., Zlatanova, S., Alattas, A.F.M. and Li, K.J., 2020. Towards indoorGML 2.0: updates and case study illustrations. *Int. Arch. Photogramm. Remote Sens. Spatial Inf. Sci*., XLIII-B4-2020: 337--344.

Diakité, A.A. and Zlatanova, S., 2018. Spatial subdivision of complex indoor environments for 3D indoor navigation. *Int. J. Geogr. Inf. Sci*., 32(2): 213-235.

Guler, D., 2024. 3D modelling of subsurface legal spaces and boundaries for 3D land administration. *Tunn. Undergr*. Space Technol., 152: 105956.

He, W., Zeng, J., Zhang, J., Namaiti, A., Shi, W., Song, Y. and Tian, J., 2025. Dynamic urban flood risk assessment based on human activity patterns: An IFAHP-EWM-TOPSIS approach. *Sust. Cities Soc*., 133: 106832.

Kakimoto, R. and Yoshida, M., 2022. Evacuation action during torrential rain considering situation awareness error using protection motivation theory. *Int. J. Disaster Risk Reduct*., 82: 103343.

Karabin, M., Kitsakis, D., Koeva, M., Navratil, G., Paasch, J.M., Paulsson, J., Vučić, N., Janečka, K. and Lisec, A., 2020. Layer approach to ownership in 3D cadastre in the case of underground tunnels. *Land Use Policy*, 98: 104464.

Karimi, H.A. and Kasemsuppakorn, P., 2013. Pedestrian network map generation approaches and recommendation. *Geogr. Inf. Syst*., 27(5): 947-962.

Koks, E.E., Jongman, B., Husby, T.G. and Botzen, W.J.W., 2015. Combining hazard, exposure and social vulnerability to provide lessons for flood risk management. *Environ. Sci. Policy*, 47: 42-52.

Kray, C., Fritze, H., Fechner, T., Schwering, A., Li, R. and Anacta, V.J., 2013. Transitional spaces: between indoor and outdoor spaces. *Spatial Information Theory. COSIT 2013. Lecture Notes in Computer Scienc*, Springer International Publishing, Cham, pp. 14-32.

Lei, B., Janssen, P., Stoter, J. and Biljecki, F., 2023. Challenges of urban digital twins: a systematic review and a Delphi expert survey. *Autom. Constr.*, 147: 104716.

León, J., Ogueda, A., Hurtado, L., Gubler, A. and Zamora, N., 2025. An integrated framework for analysing horizontal and vertical tsunami evacuation. A case study of Iquique, Chile. *Int. J. Disaster Risk Reduct.*, 116: 105137.

Lindell, M.K. and Perry, R.W., 2012. The protective action decision model: Theoretical modifications and additional evidence. *Risk Anal.*, 32(4): 616-632.

Lindell, M.K., Arlikatti, S. and Huang, S., 2019. Immediate behavioral response to the June 17, 2013 flash floods in Uttarakhand, North India. *Int. J. Disaster Risk Reduct.*, 34: 129-146.

Liu, S., Murray-Tuite, P. and Schweitzer, L., 2012. Analysis of child pick-up during daily routines and for daytime no-notice evacuations. *Transp. Res. A: Policy Pract*, 46(1): 48-67.

Luo, Z., Tian, J., Zeng, J. and Pilla, F., 2024. Flood risk evaluation of the coastal city by the EWM-TOPSIS and machine learning hybrid method. *Int. J. Disaster Risk Reduct.*, 106: 104435.

Lv, W., Deng, F., Wang, J., Han, Y. and Yang, S., 2025. Large-scale real-time evacuation modeling during urban floods: A coupled agent-based multi-model framework. *Simul. Model. Pract. Theory*, 140: 103075.

Maranzoni, A., D'Oria, M. and Rizzo, C., 2023. Quantitative flood hazard assessment methods: A review. J. *Flood Risk Manag.*, 16(1): e12855.

Mizumura, T., Taguchi, H. and Nakamura, H., 2024. Confirming the safety improvement and evacuation time reduction effects by the method for evacuating inundated areas via the shortest possible route. *Int. J. Disaster Risk Reduct.*, 101: 104252.

Morss, R.E., Mulder, K.J., Lazo, J.K. and Demuth, J.L., 2016. How do people perceive, understand, and anticipate responding to flash flood risks and warnings? Results from a public survey in Boulder, Colorado, USA. *J. Hydrol.*, 541: 649-664.

Mostafizi, A., Wang, H., Cox, D. and Dong, S., 2019. An agent-based vertical evacuation model for a near-field tsunami: Choice behavior, logical shelter locations, and life safety. *Int. J. Disaster Risk Reduct.*, 34: 467-479.

Mostafizi, A., Wang, H., Cox, D., Cramer, L.A. and Dong, S., 2017. Agent-based tsunami evacuation modeling of unplanned network disruptions for evidence-driven resource allocation and retrofitting strategies. *Nat. Hazards*, 88(3): 1347-1372.

Ringo, J., Sabai, S. and Mahenge, A., 2024. Performance of early warning systems in mitigating flood effects. A review. *J. Afr. Earth Sci.*, 210: 105134.

Nakai, F., Wise, S., Nakanishi, H., Han, W., Nakamura, S., Otsuyama, K., Kei, T., and Sekimoto, Y., 2026. Toward Smart City Digital Twins: Bridging Preparation and Response Phases in Urban Flood Evacuation through Agent-Based Modeling. In *Proceedings of the 59th Hawaii International Conference on System Sciences*, pp. 1841–1850.

OGC Consortium., 2021. Open Geospatial Consortium CityGML.

Roy, K.C., Hasan, S., Abdul-Aziz, O.I. and Mozumder, P., 2022. Understanding the influence of multiple information sources on risk perception dynamics and evacuation decisions: An agent-based modeling approach. *Int. J. Disaster Risk Reduct.*, 82: 103328.

Ryan, B., 2018. Establishing information seeking pathways in slow and flash floods. *Int. J. Disaster Risk Reduct.*, 31: 9-19.

Shu, X., Ye, C., Xu, Z., Liao, R. and Zhang, S., 2025. A multiscale physically-based approach to urban flood risk assessment using ABM and multi-source remote sensing data. *Int. J. Disaster Risk Reduct.*, 119: 105332.

Siam, M.R.K., Wang, H., Lindell, M.K., Chen, C., Vlahogianni, E.I. and Axhausen, K., 2022. An interdisciplinary agent-based multimodal wildfire evacuation model: Critical decisions and life safety. *Transp. Res. D: Transp. Environ*, 103: 103147.

Sun, G., Webster, C. and Zhang, X., 2019. Connecting the city: A three-dimensional pedestrian network of Hong Kong. *Environ. Plan. B: Urban Anal. City Sci.*, 48(1): 60-75.

Wang, Y., Kyriakidis, M. and Dang, V.N., 2021. Incorporating human factors in emergency evacuation – An overview of behavioral factors and models. *Int. J. Disaster Risk Reduct.*, 60: 102254.

Wang, Z., Zlatanova, S., Mostafavi, M.A., Khoshelham, K., D I Az-Vilari No, L. and Li, K.J., 2023. Automatic generation of routing graphs for indoor-outdoor transitional space to support seamless navigation. *ISPRS Ann. Photogramm. Remote Sens. Spatial Inf. Sci*, X-1/W1-2023: 487--492.

Weller, S.C., Baer, R. and Prochaska, J., 2016. Should I Stay or Should I Go? Response to the Hurricane Ike Evacuation Order on the Texas Gulf Coast. *Nat. Hazards Rev.*, 17(3): 04016003.

Xie, R., Zlatanova, S., Aleksandrov, M. and Lee, J.B., 2024. A voxel-based 3D indoor model to support 3D pedestrian evacuation simulations. *J. Build. Eng.*, 98: 111183.

Xie, R., Zlatanova, S. and Lee, J.B., 2025a. Simulating 3D pedestrian motions in evacuations under high and low perceived urgency levels. *Dev. Built Environ.*, 23: 100724.

Xie, R., Zlatanova, S. and Lee, J.B., 2025b. The Influence of 3D Motions on the Efficiency of Children's Indoor Evacuations. *ISPRS Ann. Photogramm. Remote Sens. Spatial Inf. Sci*, X-4/W6-2025: 233--240.

Xie, R., Zlatanova, S. and Lee, J.B., 2022. 3D indoor-pedestrian interaction in emergencies: A review of actual evacuations and simulation models. *Int. Arch. Photogramm. Remote Sens. Spatial Inf. Sci*, XLVIII-4/W4-2022: 183--190.

Xie, R., Zlatanova, S., Lee, J.B. and Aleksandrov, M., 2023. A motion-based conceptual space model to support 3D evacuation simulation in indoor environments. *ISPRS Int. J. Geo-Inf.*, 12(12), 494.

Xie, R., Zlatanova, S., Lee, J.B., and Borrmann, A., 2025c. Evacuation Behavioural Instructions with 3D Motions: Insights from Three Use Cases, *ISPRS Int. J. Geo-Inf.*, 14(5), 197.

Yan, J., Diakité, A.A. and Zlatanova, S., 2019. A generic space definition framework to support seamless indoor/outdoor navigation systems. Trans. Gis, 23(6): 1273-1295.

Yang, L., Wang, X., Zhang, J.J, Zhou, M., and Wang, F., 2020. Pedestrian Choice Modeling and Simulation of Staged Evacuation Strategies in Daya Bay Nuclear Power Plant. *IEEE Trans. Comput. Soc. Syst.*, 7(3): 686-695.

Yang, Y., Yin, J., Feng, W., Yang, L.E. and Wang, J., 2025. Dynamic flood evacuation modelling for coastal cities: A case study of Shanghai. *Int. J. Disaster Risk Reduct.*, 125: 105591.

Yuan, S., Chun, S.A., Spinelli, B., Liu, Y., Zhang, H. and Adam, N.R., 2017. Traffic evacuation simulation based on multi-level driving decision model. *Transp. Res. C: Emerg. Technol*, 78: 129-149.

Zlatanova, S., Yan, J., Wang, Y., Diakité, A.A., Isikdag, U., Sithole, G. and Barton, J., 2020. Spaces in Spatial Science and Urban Applications—State of the Art Review. *ISPRS Int. J. Geo-Inf.*, 9(1), 58.